Optimization of Carvacrol Nanoemulsion for the Incorporation in Pectin Membranes: Influence on Their Load Capacity, Microstructure and Antibacterial Properties

O. Beltrán[a], M. Luna[a], E. Valbuena-Gregorio[b], R. G. Valdez-Melchor[b], S. E. Burruel-Ibarra[c],

L. Quihui-Cota[d], S. Ruiz-Cruz[e], J. Juárez[a], M. A. López-Mata[b]* (ORCID)

[a]Universidad de Sonora, Departamento de Física, Posgrado en Nanotecnología, Unidad Centro, Hermosillo, Sonora, México.
[b]Universidad de Sonora, Departamento de Ciencias de la Salud, Campus Cajeme. Blvd. Bordo Nuevo s/n, Antiguo Providencia, Cd. Obregón, Sonora, México.
[c]Universidad de Sonora, Departamento de Investigación en Polímeros y Materiales, Unidad Centro, Hermosillo, Sonora, México.
[d]Centro de Investigación en Alimentación y Desarrollo, Coordinación de Nutrición, Departamento de Nutrición Pública y Salud, A.C. Carretera Gustavo Enrique Astiazarán Rosas, No. 46. Col. La Victoria, Hermosillo, Sonora, México.
[e]Universidad de Sonora, Departamento de Investigación y Posgrados en Alimentos, Unidad Centro, Hermosillo, Sonora, México.

Interest in developing novel wound dressings with antibacterial properties elaborated from natural sources continues to grow. In this study, a Tween-80 (T80)-stabilized carvacrol (CAR) emulsion was incorporated into pectin (PEC) membranes at 0 (control), 0.25, 0.50, and 1.00% (v/v). Membranes were obtained by the dry-casting method, characterized by scanning electron microscopy, infrared spectroscopy, and CAR retention (HPLC), and tested for antibacterial activity. The retention percentage of CAR in the membranes ranged from 9.1-13.9%. Infrared spectra analysis indicated changes in the hydrogen bonds of the membranes that suggest an interaction between the polymer matrix and the CAR:T80 emulsion. Microstructural analysis of the membranes showed the presence of hole-like features on the surface ($\approx$ 4-6 μm diameter) that indicate entrapment of the micelles in the matrix (microcapsules). The PEC-CAR membranes exhibited antibacterial activity against *Escherichia coli* and *Staphylococcus aureus*, two pathogens commonly associated with wounds and intra-hospital infections.

Keywords: *pectin, membrane, emulsion, carvacrol, antibacterial.*

1. Introduction

Most compounds obtained from essential oils like cinnamaldehyde, thymol, and carvacrol (CAR), have drawn attention due to their biological properties[1]. CAR is a phenolic monoterpenoid [2-methyl-5-(1-methylethyl) phenol] obtained primarily from oregano (*Origanum vulgare* L.) and thyme (*Thyme vulgaris* L.) essential oils[2]. It has been widely used in the food and cosmetic industries (as a flavoring and preservative, and fragrance, respectively), but recent *in vitro* and *in vivo* studies suggest its potential use in clinical applications because of its antimicrobial, antioxidant, anticancer, anti-inflammatory, hepatoprotective, spasmolytic, and vasorelaxant properties[3-5]. However, CAR is highly volatile, shows hydrophobicity, is labile to air and temperature, and is very irritating when applied in high concentrations directly on animal tissues. Hence, an encapsulation system based on a biopolymer with the ability to preserve and take better advantage of its properties is required to increase its potential clinical applications[3]. Biopolymers like starch,

cellulose, alginate[6], chitosan and pectin (PEC)[7,8] are often used for the encapsulation and controlled delivery of bioactive compounds. PEC has been used to protect and enhance the stability of diverse bioactive compounds in order to increase their lifespan and biological activity[9,10]. Chemically, PEC is a nonlinear, anionic heteropolysaccharide extracted from citrus peel. The backbone of this biopolymer consists mainly of *D*-galacturonic acid (chains of 300-1000 units) bonded by α-(1-4) with side chains of neutral carbohydrates, such as arabinan, galactan, and arabinogalactan, linked by α-(1-2) bonds. Other sugars that may be linked to the lateral chains are *D*-xylose, *D*-glucose, *D*-mannose, *L*-fucose, and *D*-galacturonic acids[11]. PEC is recognized as a low-cost biomaterial with biocompatibility, biodegradability, and film-forming properties[12]. These characteristics have been explored to elaborate wound dressings[13] and other biomaterials with biomedical applications[14].

When applied on damaged tissue, wound dressings are recognized as dynamic, complex materials since their components interact with various cell strains, molecules, and environments to repair the tissue and maintain aseptic

conditions[15]. Therefore, novel wound dressings loaded with antibacterial compounds are being developed, as well as drug delivery systems designed to inhibit the proliferation of microorganism and accelerate healing[16]. The global market associated with biomaterials for wound care is growing. Indeed, economic studies valued this market in $18.22 billion dollars in 2016 with an expected increase of 5% ($26.24 billion) by 2023[17,18]. This economic growth is due to the high incidence of hospital-acquired infections associated with antibiotic-resistant microorganisms. For instance, *Staphylococcus aureus* (*S. aureus*) and *Escherichia coli* (*E. coli*) are recognized as being responsible for 80% of wound infections and as the most common causes of hospital-acquired infections by antibiotic-resistant microorganisms[19,20]. The present study suggests that CAR can be used as an alternative natural therapeutic compound because of its antibacterial activity against these two bacteria. Previous works have reported various ways of preserving CAR in a PEC matrix by incorporating it directly into the matrix without adding a surfactant[21], by adding a surfactant to the polysaccharide followed by CAR[22], or by preparing a CAR-surfactant emulsion that is added to a polysaccharide matrix solution for encapsulation[23,24]. Most of those studies have reported only the stability of the emulsion during a repose time at room temperature, without mentioning the proportions of the surfactant and bioactive compound, while others failed to report the droplet size during incorporation or encapsulation[25]. Stabilization of the nanoemulsions using suitable amounts of surfactant and an oil phase has been suggested as a way to improve the biological activity of bioactive compounds[26]. The surfactant most often used to prepare emulsions is Tween 80 [T80, polyoxyethylene sorbitan monooleate]. T80 is a nonionic amphiphilic molecule, usually safe, with two segments: a nonpolar tail and a hydrophilic head. When T80 is added to an oil-water mixture, the nonpolar tail (hydrophobic segment) is incorporated into the oil phase, while the polar head (hydrophilic segment) interacts with the surrounding aqueous phase to form an emulsion[27]. Based on this, the optimal organization of T80 molecules with an oil phase (like CAR) may reduce molecular interaction with the PEC matrix. Studies have also documented that polysaccharide hydrogels can form a thick layer on oil droplets that are stabilized by steric repulsion[28,29]. In our view, by optimizing the amounts of CAR and T80 during elaboration of a nanoemulsion, the droplet size can be controlled, allowing their later incorporation into the PEC hydrogel to form a membrane with encapsulated CAR that could function as a suitable antibacterial wound dressing. Therefore, the aims of this study were (1) to obtain a stabilized emulsion by optimizing the amounts of CAR and T80, and (2) to elaborate and evaluate the physicochemical and antibacterial properties of PEC membranes loaded with CAR using the dry casting method.

2. Materials and Methods

2.1. Materials

PEC with ≈ 65% of *D*-galacturonic acid was provided by Química Suastes, S.A. de C.V. (Chemical Meyer Reactive, Mexico). CAR (98% purity), glycerol (99% purity), and polyoxyethylene sorbitan monooleate [Tween 80® (T80)],

a non-ionic detergent, were purchased from Sigma-Aldrich (Missouri, USA). All chemicals used were of reagent grade or higher quality.

2.2. CAR:T80 emulsions

CAR:T80 emulsions were prepared by the sonication method, maintaining the amount of T80 (T80 1.0% v/v) constant but systematically varying the CAR volume to obtain the following CAR:T80 ratios: 0:1, 1:16, 1:8, 1:4, and 1:2 (m:m). During preparation of the emulsions samples were maintained in a cold-water bath (4ºC) with a short processing time (5 min) to reduce loss due to temperature changes. The optimal amount of CAR loaded into the core of the T80 micelles and expressed as the maximum CAR-load capacity of the micelle was determined in relation to the size and stability of the emulsion. First, hydrodynamic radius of micelles was determined by dynamic light-scattering (DLS) at an angle of 90º (ALV-5000/E, ALV Gmbh, Germany). The CONTIN method[30] was then used to analyze the scattered light. The diffusion coefficient was determined from the decay rates ($\Gamma = Dq^2$) which were j$e^{-\Gamma \tau}$. The micelle size was then determined by the Stokes-Einstein equation:

$$D_h = \frac{\kappa_B T}{3\pi\eta D}$$

(1)

where κ_B, T, and η are the Boltzmann constant, absolute temperature, and solvent viscosity, respectively. Results are presented as the average diameter of the droplets (d32) using the Sauter diameter expression and calculated as follows: $d_{32} = \sum_i nidi^3 / \sum_i nidi^2$; where *ni* is the number of droplets between consecutive diameters (*di*)[31].

2.3. Preparation of PEC membranes loaded with CAR

A PEC solution (6.0% m/v) was prepared under magnetic stirring (Kitlab, AM-3C, USA) at 80 RPM for 30 min at 40°C, then 4 mL of glycerol were added to the solution (100 mL) and mixed constantly for 5 min. Finally, different amounts of a previously selected CAR:T80 (1:4) emulsion (0.25, 0.5, and 1.00% v/v) were added to a PEC-glycerol mixture (10 g), adding water to complete 20 g of the mixture. The membrane was prepared by the dry-casting method, pouring 20 g of the suspension into a glass Petri dish and placing it in an oven to dry at 40°C (Binder-FD53, Germany). The dried membranes were detached from the glass Petri dish and stored in a desiccator until analysis (NaBr, 52% relative humidity) at 25°C.

2.4. Attenuated total reflection-Fourier transform infrared spectroscopy (ATR-FTIR)

Each membrane sample (5 mg) was scanned at a resolution of 2 cm⁻¹ over a wavenumber region of 400-4000 cm⁻¹ using an ATR-FTIR Perkin-Elmer 1600 spectrophotometer (Massachusetts, USA). Each measurement was performed in triplicate in transmittance mode. The degree of esterification (ED) of the PEC was estimated at 38.2%, using the ratio of the absorbance area that corresponded to the ester-carbonyl bands[32].

Optimization of Carvacrol Nanoemulsion for the Incorporation in Pectin Membranes: Influence on Their Load Capacity, Microstructure and Antibacterial Properties

3

2.5. Scanning electron microscopy (SEM)

The microstructure of the membranes was analyzed using a scanning electron microscope (JEOL JSM-5410LV) [Tokyo, Japan] operated at 20 kV. The membranes were cut to a 0.5 x 0.5 cm size and placed on a cylindrical copper support (1 cm in diameter). For SEM analysis, the surface of the membrane was coated with gold to allow electric conduction and prevent the accumulation of charge under electron bombardment[33].

2.6. CAR retention in the PEC membrane

The CAR loaded in the membrane was evaluated by HPLC (Agilent, 1100 serial, California, USA) using a Zorbax Eclipse XDB-C18 column (80Å, 5µm particle, 4.6 x 250 mm, California, USA). Acetonitrile:water (50:50 v/v) was used as the mobile phase at a flow rate of 1 mL/min. The CAR samples injected were prepared as follows: first, the PEC-CAR membranes (2 x 2 cm; CAR; 0.25, 0.50, and 1.00%) were placed in an empty dialysis bag and then in a glass beaker with 15 mL of water for 24 h to separate the PEC from the CAR and avoid interference during measurement[34,35]. After that, 10 µL of the sample were injected and absorbance was monitored at 274 nm with a UV-Visible detector[36]. All analyses were performed in triplicate with a variation coefficient <5%. The CAR curve was determined ($R^2 = 0.989$). Results are expressed as the retention efficiency percentage (%RE) of CAR encapsulated into PEC membranes using the following Equation 2:

$$\%RE = \left(\frac{Amount\ of\ encapsulated\ CAR}{Total\ amount\ of\ CAR} \right) 100 \qquad (2)$$

2.7. Antibacterial activity

The antibacterial activity of the PEC-CAR membranes was evaluated against strains of *Escherichia coli* O157:H7 (ATCC 43890) and *Staphylococcus aureus* (ATCC 65384) as Gram-negative and Gram-positive bacterial models, respectively. A loopful of bacteria, preserved at -40ºC in brain-heart infusion broth (BHI) and glycerol (20%) was transferred to BHI culture media (10 mL) and incubated at 37ºC overnight. Then a loopful of this bacteria culture was transferred to BHI and incubated at 37ºC to obtain 10^6 cfu/mL. The antibacterial test was performed by the agar diffusion method, streaking 100 µL of each strain over the agar surface of Mueller-Hinton agar plates (Difco, USA). Then 6 mm-membrane-discs of PEC-CAR, PEC-T80 (1.00%), imipenem sensi-disc-10 µg-BD (positive control), and filter paper with BHI (negative control) were placed on the surface-streaked plates and incubated at 37°C for 24-48 h. The results of the antibacterial activity are expressed as the inhibition area in cm². All analyses were tested in triplicate on different assays. The inhibition areas were determined using ImageJ software, and developed at the National Institutes of Health, USA[37].

2.8. Statistical analysis

Analysis of variance was used to determine differences among the mean values. The membranes tested were used as the independent factors. The radium (nm), retention of CAR (%), and antibacterial activity were used as the response variables. Additionally, a Duncan test for multiple comparisons was used assuming an α= 0.05. All statistical analyses were performed with the NCSS statistical package, version 2000.

3. Results and Discussion

3.1. Optimal CAR-load in the T80 micelles

Figure 1 shows the image of the CAR:T80 emulsions prepared at different ratios, which changed from transparent to turbid at the naked eye. DLS analysis was used to determine the maximum amount of CAR entrapped in the T80 surfactant, considering droplet diameter. No difference was found in the diameter of the droplets in the emulsions prepared at 1:16 (9.6 ± 0.6 nm) and those with only T80 (9.8 ± 0.2 nm) (p > 0.05). This suggests that the amount of CAR added to the system was insufficient to propel a change of thermodynamic forces of T80 to form full micelles[38]. However, droplet diameter increased significantly (p<0.05) at the proportion of 1:8 (12.6 ± 0.2 nm), suggesting that this is the minimum amount of CAR required to induce optimization of the curvature for micelle formation[39]. The emulsion with the 1:4 ratio appeared slightly cloudy to the naked eye, while the droplet diameter of the micelles (140.2 ± 0.8 nm) suggests a saturation of the CAR loaded into the micelle formed by T80. Hence, this emulsion showed high stability and low polydispersity. The diameter of the micelles increased significantly (1436 ± 150 nm) at the highest CAR:T80 ratio (1:2), and sediment from the CAR:T80 emulsion was observed at the bottom of the recipient as time passed. This suggests that emulsion system saturation occurred, since a high number of T80 molecules is required to cover the entire surface of the micelles, though this may result in an increased droplet size[27].

Based on these results, the emulsion prepared at the 1:4 ratio was selected to prepare the PEC-CAR membrane, since it is highly stable and the nanoparticle size was within the range recommended for biomedical applications[40,41]. Images of the membranes obtained showed a transparent appearance
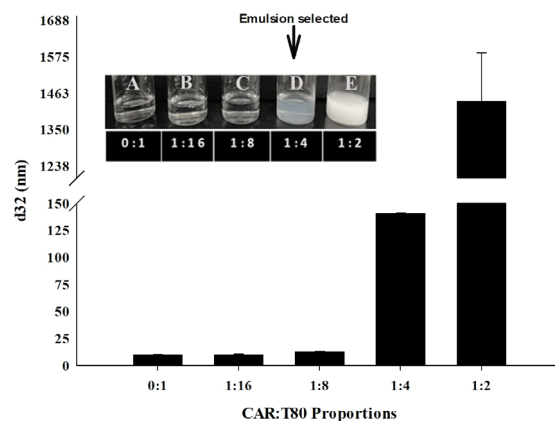

Figure 1. Diameter droplets of the micelles of CAR:T80 emulsions after preparation. The image show the visual appearance of the emulsions where; (**A**) Control, (**B**) 1:16, (**C**) 1:8, (**D**) 1:4 and (**E**) 1:2 of CAR:T80 proportions.

(Figure 2). This is an important property because it allows the wound to be visualized without removing the dressing[42].

3.2. Scanning electron microscopy (SEM)

The SEM images show the presence of aggregates and crystal-like structures of diverse sizes and branched shapes on the surface membranes (Figure 3). The PEC membrane prepared with only T80 (1.0%) showed crystal-like aggregates with a size around 800 nm (Figure 3, A0 and A1). Those structures on the surface of the PEC membrane may be composed mostly of T80 due to its expulsion from the interior of the PEC membrane to the surface that occurs during the dry-casting process[43]. Cardiel et al.[43] documented that the micelles of the surfactant mediate the nucleation sites, promoting the crystallization of T80. Meanwhile, the PEC-CAR 0.25 (Figure 3, B0 and B1) and 0.50% (Figure 3, C0 and C1) microstructures showed smaller crystal-like aggregates and hole-like features on the surface ($\approx$ 4-6 µm diameter), likely as a result of the disintegration of the CAR:T80 microcapsules during dry-casting. Similarly, the presence of the microcapsule on the surface of the PEC-CAR membranes may have resulted from the disruption and restructuring of the CAR:T80 micelles during mixing with the PEC matrix solution[28] and the water evaporation that occurs during dry-casting, where the coalescence of the CAR:T80 micelles is induced[44]. Although the droplet diameter of the emulsion incorporated initially into the PEC matrix was within the nanometric scale for micelles (140.2 ± 0.8 nm), the presence of the microcapsule on the surface suggests an increase of micelle size during the process of membrane elaboration that may be associated with the following two events. First, water loss in the PEC matrix probably induced a reduction of the distance among the emulsion droplets dispersed in the membrane-forming solution, which not only increased the probability of collisions, but was followed by an increase in droplet size (coalescence pathway) during the drying process[44]. The second event may be associated with the homogenization process of PEC-CAR, which induces a disruption of the emulsion and separation of the components (CAR and T80), associated with interactions between the hydrophobic sites of the PEC structure and the CAR (emulsion), together with the restructuring of the CAR:T80 emulsion[28]. The microstructure of the 1.00% PEC-CAR membrane (Figure 3, **D0 and D1)** showed an

excess of crystal-like aggregates on the surface due to the high addition of CAR:T80. It has been suggested that the process of micellar growth induced by T80 forms nucleation sites that may encapsulate CAR inside the crystals, reported as well by Cardiel et al.[43] Recently, nano- and microcrystals with hydrophobic compounds have been elaborated with polysaccharides and nonionic surfactants in diverse shapes and sizes[45,46].

3.3. FTIR-ATR

Figure 4 shows the infrared spectra of the PEC membranes loaded with and without CAR. The absorption bands centered around 3300 cm^{-1} were assigned to the stretching vibration of -OH groups. The width and intensity of the transmittance band may be associated with intermolecular interactions between the polysaccharide chains of the PEC through the formation of inter- and intramolecular hydrogen bonds (PEC-PEC), as reported previously[47]. The peaks at 2900 cm^{-1}, 1750 cm^{-1}, 1430 cm^{-1}, and 1010 cm^{-1} were assigned to -CH$_2$-, -C=O, -C-O-C- and -CH- groups, respectively, of the pyranose ring of PEC monomers. T80 shows bands at 2900 and 2855 cm^{-1} that correspond to CH$_3$- and -CH$_2$- aliphatic groups. A peak centered at 1750cm^{-1} and a small band at 1650 cm^{-1} correspond to -C=O and -CH=CH- groups, respectively, that are intrinsic to the aliphatic chain of the surfactant. The small band at 1110 cm^{-1} corresponds to the ester bond (-CO-O-) of the surfactant[48]. It is important to note that the functional groups of the organic compounds used in elaborating the membrane (PEC, T80, CAR) are similar, so the absorption bands should overlap at the same wavenumber. In this regard, the FTIR spectrum recorded for the PEC-CAR membrane showed overlapping of the transmittance bands and peaks of their respective functional groups, as has been observed recently for PEC/*Aloe*-gel film loaded with CAR[49]. However, the presence of T80 or CAR:T80 entrapped in the PEC membrane was evidenced by comparing the intensity changes of the bands at 3300, 2900, and 1110 cm^{-1}, which corresponded to hydroxyl, aliphatic, and ester functional groups, respectively. The decrease in the band intensity at 3300 cm^{-1}, seen in Figure 4, suggests that the T80 entrapped in the PEC membrane disrupts the hydrogen bonds between PEC-PEC, thus modifying the structure of the membrane, while an increase in the intensity of peaks, attributed to aliphatic and ester groups, was observed. The presence of
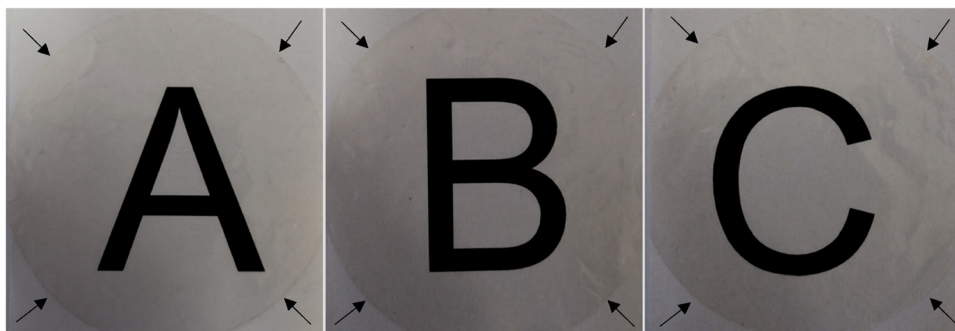

Figure 2. Picture of the membranes of PEC-CAR 0.25% (**A**), PEC-CAR 0.50% (**B**) and PEC-CAR 1.00% (**C**). Black arrows indicate the outline of the membranes.
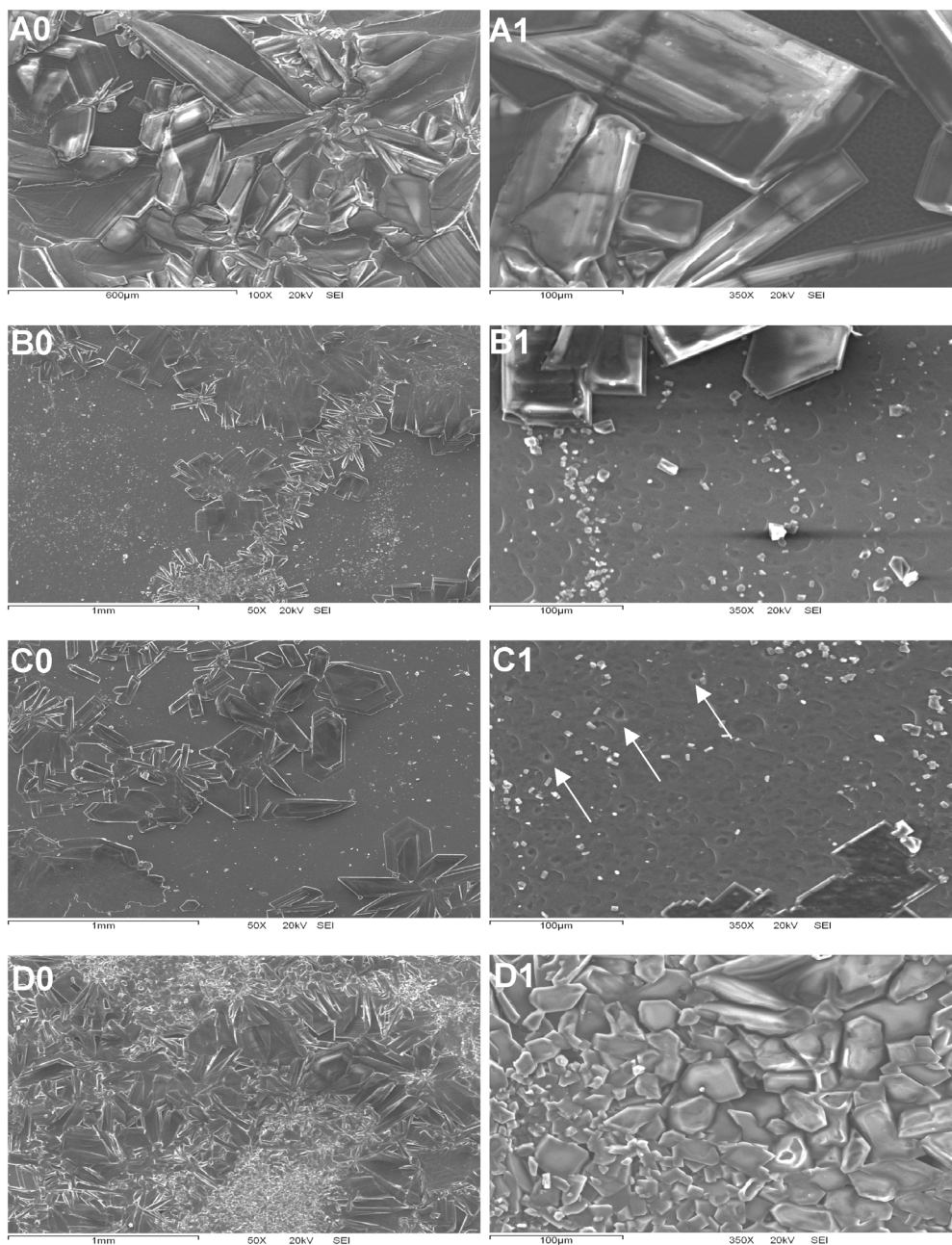
Figure 3. SEM images of PEC membranes: control PEC membranes only with T80 1.0% (A0 and A 1), PEC-CAR 0.25% (B0 and B1), PEC-CAR 0.50% (C0 and C1) and PEC-CAR 1.00% (D0 y D1) (Each one of them were amplified 50X and 350X, respectively). White arrows indicate the presence of hole on membrane surface.

CAR in the PEC membranes was evidenced by the increased intensity of the hydroxyl band compared to the PEC-T80 control, though the intensity of this band decreased as the proportion of CAR increased. For instance, the PEC-CAR membrane prepared at the lowest proportion of CAR:T80 (0.25%) showed a higher absorption intensity than that observed at the 0.50 and 1.0% proportions of CAR:T80. This suggests that the CAR:T80 emulsion was entrapped in the PEC membrane, as evidenced by the formation of microcapsules revealed by SEM micrograph.

3.4. CAR retention in the membrane

Figure 5 shows the percentage of CAR entrapped in the PEC membrane. The 0.50% PEC-CAR membrane had the highest retention percentage (13.89%) followed by the 0.25% (9.68%), and 1.00% membrane (9.11%). In contrast, when other polysaccharide films were used to load the CAR –chitosan[50] and PEC-alginate films[51], for instance they retained CAR more efficiently (47-48 and 77%, respectively), supporting the notion that CAR retention in polymeric matrices can vary depending on the encapsulation method
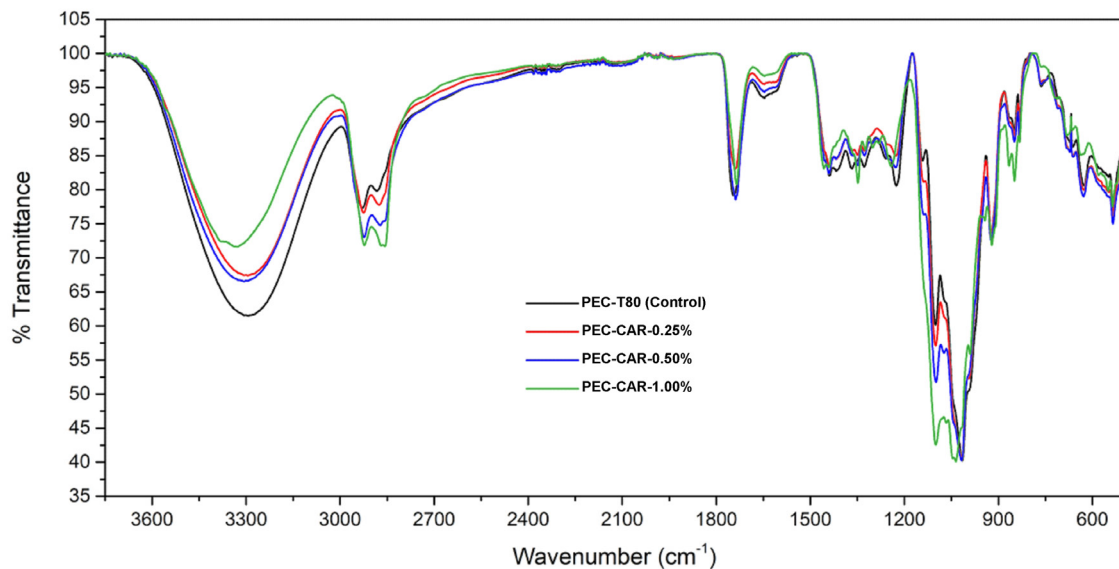
Figure 4. Infrared spectrum of PEC membranes with and without CAR (control).
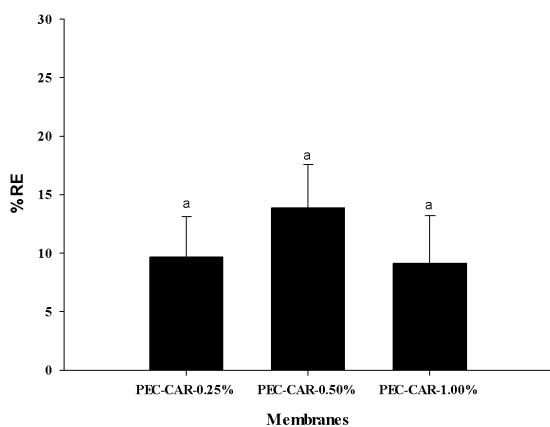

Figure 5. Encapsulation efficiency (%) in PEC-CAR membranes. *Duncan´s multiple comparison test: different letters by column indicate significant differences ($p < 0.05$).

used[52,53]. The low percentages of CAR retention reported in this study could be influenced by the dialysis method used. Maryam et al.[54] evaluated the release profile of CAR from a system of CAR-loaded human serum albumin nanoparticles that also used the dialysis method during 240 h. They found that the amount of CAR released in 24 h was 40.4% and that CAR release reached a maximum of 79.5% between 192 and 240 h. Another study based on the preparation of beeswax solid nanoparticles loaded with CAR and astaxanthin also determined the rate of CAR release. During a phase of 1-3 h, release was 16.2% and 6.89%, and this continued after 168 h, indicating a gradual release of CAR into the aqueous medium under the dialysis method[55]. Two limitations of our study are that the kinetic release of CAR from the membranes was not evaluated, and the low percentage of retention found could represent only one point of the release.

The gradual release of CAR may be advantageous because high concentrations of CAR administered topically can cause tissue irritation[56], while evidence of its use in wound healing suggests that a low concentration (≈5%) of an *Origanum* essential oil emulsion (83% CAR) is recommendable[53]. In addition, the low percentage of CAR retention observed in this study may reduce the probability of irritation during its application as a wound dressing. However, further studies are required to determine the standard posology.

3.5. Antibacterial activity

The antibacterial activity of the PEC-CAR membranes was evaluated against *E. coli* O157:H7 and *S. aureus*, two bacteria commonly associated with both wound and hospital-acquired infections (Table 1). All the PEC membranes loaded with CAR showed some antibacterial activity against *E. coli* O157:H7, but PEC-CAR at 1.00% had the highest activity, followed by the 0.50 and 0.25% membranes ($p < 0.05$). *S. aureus* showed similar inhibition to the 0.50 and 1.00% PEC-CAR membranes ($p > 0.05$). The authors consider that the antibacterial activity of PEC-CAR could have been underestimated due to certain phenomena that may have occurred during the antibacterial assays, strongly associated with the chemical nature of CAR (hydrophobic and volatile) when placed on an aqueous surface like agar medium: i) when the PEC-CAR membranes contacted the surface of the agar, water in the medium may have induced swelling and the later solubilization of the membranes, releasing the CAR encapsulated in the PEC matrix[28]. However, only a small amount of CAR could have diffused onto the agar due to its low solubility in the aqueous medium which limits its antibacterial action[57]. Tampau et al.[58] also reported that the release of CAR into an aqueous system compromises its antibacterial activity despite the adequate load revealed in a system of electrospun poly-(ε-caprolactone) fiber mats with encapsulated CAR. The limitations of CAR diffusion on agar medium have been reported by other authors[59,60].

Optimization of Carvacrol Nanoemulsion for the Incorporation in Pectin Membranes: Influence on Their Load Capacity, Microstructure and Antibacterial Properties

7

Table 1. Growth inhibition exhibited by *E. coli* and *S. aureus* in the presence of CAR-PEC membranes.

Membranes and controls	Inhibitory area (mm^2)	
	E. coli O157:H7*	*S. aureus**
Filter paper (Control)	NI**	NI
PEC-T80-1.00% (Control)	NI	NI
PEC-CAR-0.25%	0.88 ± 0.06^a	NI
PEC-CAR-0.50%	1.63 ± 0.07^b	1.37 ± 0.17^a
PEC- CAR-1.00%	2.43 ± 0.13^c	1.64 ± 0.25^a

*Duncan's multiple comparison test: different superscript letters by column indicate significant differences ($p < 0.05$). **NI= No inhibition.

Figure 6. An example of the irregular inhibition halos showed on Mueller-Hinton agar (*Escherichia coli* O157:H7) and absence of the disk (6 mm) of the PEC-CAR membrane because of its dissolution. *Triplicate inhibition halos on the right side of plate (PEC-CAR-1.00%) and left side of plate (PEC-T80-control).

ii) Antibacterial activity may be related to the volatile nature of CAR, which can act on the culture medium in a vapor state that affects the survival of bacteria[61]. Some studies have considered evaluating the antimicrobial activity of CAR in vapor states[62-64]. Their findings indicate that CAR can act in a dual way during antibacterial activity on solid culture medium (liquid and vapor state). This phenomenon may explain the presence of the areas of irregular inhibition observed in the medium (Figure 6). It is also important to note that the presence of CAR in the crystals observed on the surface of the membranes, evidenced by SEM analysis, probably affected its antibacterial activity, though the concentration in those crystals was not determined. The PEC-CAR membranes showed less antibacterial activity against *S. aureus* than *E. coli*, likely associated with the composition of the cell wall of the bacteria. The cell wall of Gram-positive bacteria is thick and made up of several layers of peptidoglycan, while the cell wall of Gram-negative bacteria is thin with less peptidoglycan. Apparently, the effect of CAR is greater on cell membranes with low concentrations of peptidoglycan[65], associated with changes in cytoplasm

pH that generate reactive oxygen species which inhibit the efflux pump of the bacteria[66].

4. Conclusion

The PEC-CAR membranes had a transparent appearance, and microstructural analysis evidenced the presence of microcapsules and crystal aggregates on their surface. The maximum percentage of CAR retained in the PEC membranes was 13%. The changes in the intensity of the hydroxyl band in the FTIR spectrum evidenced the presence of CAR in the PEC membranes. The amount of CAR retained in the membranes was sufficient to inhibit the growth of *E. coli* and *S. aureus.* The PEC-CAR membrane thus showed potential for use as a biomaterial in the elaboration of wound dressings, though additional studies on this topic are required.

5. Acknowledgments

6. References

1. Wei Z, Huang Q. Assembly of protein-polysaccharide complexes for delivery of bioactive ingredients: a perspective paper. J Agric Food Chem. 2019;67(5):1344-52.
2. Vincenzi M, Stammati A, De Vincenzi A, Silano M. Constituents of aromatic plants: carvacrol. Fitoterapia. 2004;75(7-8):801-4.
3. Sharifi-Rad M, Varoni EM, Iriti M, Martorell M, Setzer WN, del Mar Contreras M, et al. Carvacrol and human health: a comprehensive review. Phytother Res. 2018;32(9):1675-87.
4. Suntres ZE, Coccimiglio J, Alipour M. The bioactivity and toxicological actions of carvacrol. Crit Rev Food Sci Nutr. 2015;55(3):304-18.
5. Melo FHC, Rios ERV, Rocha NFM, Citó MCO, Fernandes ML, Sousa DP, et al. Antinociceptive activity of carvacrol (5-isopropyl-2-methylphenol) in mice. J Pharm Pharmacol. 2012;64(12):1722-9.
6. Grøndahl L, Lawrie G, Anitha A, Shejwalkar A. Applications of alginate biopolymer in drug delivery. In: Sharma C, editor. Biointegration of medical implant materials. Duxford: Elsevier; 2019. p. 375-403.
7. Keawchaoon L, Yoksan R. Preparation, characterization and in vitro release study of carvacrol-loaded chitosan nanoparticles. Colloids Surf B Biointerfaces. 2011;84(1):163-71.
8. Mendes JP, Esperança JMSS, Medeiros MJ, Pawlicka A, Silva MM. Structural, morphological, ionic conductivity, and thermal

properties of pectin-based polymer electrolytes. Mol Cryst Liq Cryst. 2017;643(1):266-73.

9. Noh J, Kim J, Kim JS, Chung YS, Chang ST, Park J. Microencapsulation by pectin for multi-components carriers bearing both hydrophobic and hydrophilic active agents. Carbohydr Polym. 2018;182:172-9.

10. Rehman A, Ahmad T, Aadil RM, Spotti MJ, Bakry AM, Khan IM, et al. Pectin polymers as wall materials for the nano-encapsulation of bioactive compounds. Trends Food Sci Technol. 2019;90:35-46.

11. Fracasso AF, Perussello CA, Carpiné D, Petkowicz CLO, Haminiuk CWI. Chemical modification of citrus pectin: structural, physical and rheologial implications. Int J Biol Macromol. 2018;109:784-92.

12. Du Le H, Loveday SM, Nowak E, Niu Z, Singh H. Pectin emulsions for colon-targeted release of propionic acid. Food Hydrocoll. 2020;103:105623.

13. Rezvanian M, Ahmad N, Mohd Amin MCI, Ng S-F. Optimization, characterization, and in vitro assessment of alginate-pectin ionic cross-linked hydrogel film for wound dressing applications. Int J Biol Macromol. 2017;97:131-40.

14. Mishra RK, Banthia AK, Majeed ABA. Pectin based formulations for biomedical applications: a review. Asian J Pharm Clin Res. 2012;5:1-7.

15. Qu J, Zhao X, Liang Y, Xu Y, Ma PX, Guo B. Degradable conductive injectable hydrogels as novel antibacterial, antioxidant wound dressings for wound healing. Chem Eng J. 2019;362:548-60.

16. Liu H, Wang C, Li C, Qin Y, Wang Z, Yang F, et al. A functional chitosan-based hydrogel as a wound dressing and drug delivery system in the treatment of wound healing. RSC Advances. 2018;8(14):7533-49.

17. MarketResearch.com. Wound Care - Global Market Outlook [Internet]. 2021 [cited 2021 Jan 27]. Available from: https://www.marketresearch.com/Stratistics-Market-Research-Consulting-v4058/Wound-Care-Global-Outlook-11369030/

18. Weller CD, Team V, Sussman G. First-line interactive wound dressing update: a comprehensive review of the evidence. Front Pharmacol. In press. https://doi.org/10.3389/fphar.2020.00155.

19. Komijani M, Bouzari M, Rahimi F. Detection of TEM, SHV and CTX-M antibiotic resistance genes in *Escherichia coli* isolates from infected wounds. Med Lab J. 2017;11:30-5.

20. Wolters M, Frickmann H, Christner M, Both A, Rohde H, Oppong K, et al. Molecular characterization of *Staphylococcus aureus* isolated from chronic infected wounds in rural Ghana. Microorganisms. 2020;8(12):2052.

21. Rodriguez-Garcia I, Cruz-Valenzuela MR, Silva-Espinoza BA, Gonzalez-Aguilar GA, Moctezuma E, Gutierrez-Pacheco MM, et al. Oregano (*Lippia graveolens*) essential oil added within pectin edible coatings prevents fungal decay and increases the antioxidant capacity of treated tomatoes. J Sci Food Agric. 2016;96(11):3772-8.

22. Yuan G, Lv H, Yang B, Chen X, Sun H. Physical properties, antioxidant and antimicrobial activity of chitosan films containing carvacrol and pomegranate peel extract. Molecules. 2015;20(6):11034-45.

23. Vilas Dhumal C, Pal K, Sarkar P. Synthesis, characterization, and antimicrobial efficacy of composite films from guar gum/sago starch/whey protein isolate loaded with carvacrol, citral and carvacrol-citral mixture. J Mater Sci Mater Med. 2019;30(10):117.

24. Sun X, Cameron RG, Bai J. Effect of spray-drying temperature on physicochemical, antioxidant and antimicrobial properties of pectin/sodium alginate microencapsulated carvacrol. Food Hydrocoll. 2020;100:105420.

25. Sun X, Cameron RG, Bai J. Microencapsulation and antimicrobial activity of carvacrol in a pectin-alginate matrix. Food Hydrocoll. 2019;92:69-73.

26. Ryu V, McClements DJ, Corradini MG, Yang JS, McLandsborough L. Natural antimicrobial delivery systems: Formulation, antimicrobial activity, and mechanism of action of quillaja saponin-stabilized carvacrol nanoemulsions. Food Hydrocoll. 2018;82:442-50.

27. Roldan-Cruz C, Vernon-Carter EJ, Alvarez-Ramirez J. Assessing the stability of Tween 80-based O/W emulsions with cyclic voltammetry and electrical impedance spectroscopy. Colloids Surf Physicochem Eng Asp. 2016;511:145-52.

28. Verkempinck SHE, Kyomugasho C, Salvia-Trujillo L, Denis S, Bourgeois M, Van Loey AM, et al. Emulsion stabilizing properties of citrus pectin and its interactions with conventional emulsifiers in oil-in-water emulsions. Food Hydrocoll. 2018;85:144-57.

29. Charoen R, Jangchud A, Jangchud K, Harnsilawat T, Naivikul O, McClements DJ. Influence of biopolymer emulsifier type on formation and stability of rice bran oil-in-water emulsions: whey protein, gum arabic, and modified starch. J Food Sci. 2011;76(1):E165-72.

30. Pecora R. Dynamic light scattering measurement of nanometer particles in liquids. J Nanopart Res. 2000;2(2):123-31.

31. Jafari SM, He Y, Bhandari B. Optimization of nano-emulsions production by microfluidization. Eur Food Res Technol. 2007;225(5-6):733-41.

32. Yavuz-Düzgün M, Zeeb B, Dreher J, Özçelik B, Weiss J. The impact of esterification degree and source of pectins on complex coacervation as a tool to mask the bitterness of potato protein isolates. Food Biophys. 2020;15(3):376.

33. Reed SJB. Electron microprobe analysis and scanning electron microscopy in geology. Cambridge: Cambridge University Press; 2005.

34. Huang T, Zhao H, Fang Y, Lu J, Yang W, Qiao Z, et al. Comparison of gelling properties and flow behaviors of microbial transglutaminase (MTGase) and pectin modified fish gelatin. J Texture Stud. 2019;50(5):400-9.

35. Christensen SH. Pectins. In: Glicksman M, editor. Food hydrocolloids. Boca Raton: CRC Press; 2020. p. 205-30.

36. Hajimehdipoor H, Shekarchi M, Khanavi M, et al. A validated high performance liquid chromatography method for the analysis of thymol and carvacrol in *Thymus vulgaris* L. volatile oil. Pharmacogn Mag. 2010;6:154-8.

37. NIH: National Institutes of Healt. ImageJ. Bethesda: NIH.

38. Deng L-L, Taxipalati M, Que F, Zhang H. Physical characterization and antioxidant activity of thymol solubilized Tween 80 micelles. Sci Rep. 2016;6(1):38160.

39. Amani A, York P, Waard H, Anwar J. Molecular dynamics simulation of a polysorbate 80 micelle in water. Soft Matter. 2011;7(6):2900.

40. Tadros TF. Emulsion science and technology: a general introduction. Weinheim: Wiley; 2009. p. 1-56.

41. McClements DJ. Critical review of techniques and methodologies for characterization of emulsion stability. Crit Rev Food Sci Nutr. 2007;47(7):611-49.

42. Tabaii MJ, Emtiazi G. Transparent nontoxic antibacterial wound dressing based on silver nano particle/bacterial cellulose nano composite synthesized in the presence of tripolyphosphate. J Drug Deliv Sci Technol. 2018;44:244-53.

43. Cardiel JJ, Furusho H, Skoglund U, Shen AQ. Formation of crystal-like structures and branched networks from nonionic spherical micelles. Sci Rep. 2016;5(1):17941. http://dx.doi.org/10.1038/srep17941.

44. Shi W-J, Tang C-H, Yin S-W, Yin Y, Yang X-Q, Wu L-Y, et al. Development and characterization of novel chitosan emulsion films via pickering emulsions incorporation approach. Food Hydrocoll. 2016;52:253-64.

45. Zhang H, Jung J, Zhao Y. Preparation and characterization of cellulose nanocrystals films incorporated with essential oil loaded β-chitosan beads. Food Hydrocoll. 2017;69:164-72.

Optimization of Carvacrol Nanoemulsion for the Incorporation in Pectin Membranes: Influence on Their Load
Capacity, Microstructure and Antibacterial Properties

9

46. Barbieri N, Sanchez-Contreras A, Canto A, Cauich-Rodriguez JV, Vargas-Coronado R, Calvo-Irabien LM. Effect of cyclodextrins and Mexican oregano (*Lippia graveolens* Kunth) chemotypes on the microencapsulation of essential oil. Ind Crops Prod. 2018;121:114-23.

47. López-Mata MA, Gastelum-Cabrera M, Valbuena-Gregorio E, Zamudio-Flores PB, Burruel-Ibarra SE, Morales-Figueroa GG, et al. Physicochemical properties of novel pectin/Aloe gel membranes. Iran Polym J Engl Ed. 2018;27(8):545-53.

48. Liu Y, Gu J, Zhang J, Yu F, Wang J, Nie N, et al. LiFePO4 nanoparticles growth with preferential (010) face modulated by Tween-80. RSC Advances. 2015;5(13):9745-51.

49. Gomez-Rodriguez GH, Lopez-Mata MA, Valbuena-Gregorio E, Melchor RGV, Campos-Garcia JC, Silva-Beltran NP, et al. Microencapsulation of carvacrol using pectin/aloe-gel as a novel wound dressing films. Curr Top Med Chem. 2018;18(14):1261-8.

50. López-Mata MA, Ruiz-Cruz S, Silva-Beltrán NP, Ornelas-Paz J, Zamudio-Flores P, Burruel-Ibarra S. Physicochemical, antimicrobial and antioxidant properties of chitosan films incorporated with carvacrol. Molecules. 2013;18(11):13735-53.

51. Sun X, Cameron RG, Bai J. Microencapsulation and antimicrobial activity of carvacrol in a pectin-alginate matrix. Food Hydrocoll. 2019;92:69-73.

52. Rostami MR, Yousefi M, Khezerlou A, Aman Mohammadi M, Jafari SM. Application of different biopolymers for nanoencapsulation of antioxidants via electrohydrodynamic processes. Food Hydrocoll. 2019;97:105170.

53. Wicochea-Rodríguez JD, Chalier P, Ruiz T, Gastaldi E. Active food packaging based on biopolymers and aroma compounds: how to design and control the release. Front Chem. 2019;7:398.

54. Maryam K, Shakeri S, Kiani K. Preparation and in vitro investigation of antigastric cancer activities of carvacrol-loaded human serum albumin nanoparticles. IET Nanobiotechnol. 2015;9(5):294-9.

55. Shakeri M, Razavi SH, Shakeri S. Carvacrol and astaxanthin co-entrapment in beeswax solid lipid nanoparticles as an efficient nano-system with dual antioxidant and anti-biofilm activities. LWT. 2019;107:280-90.

56. Costa MF, Durço AO, Rabelo TK, Barreto RSS, Guimarães AG. Effects of Carvacrol, Thymol and essential oils containing such monoterpenes on wound healing: a systematic review. J Pharm Pharmacol. 2019;71(2):141-55.

57. Ben Arfa A, Combes S, Preziosi-Belloy L, Gontard N, Chalier P. Antimicrobial activity of carvacrol related to its chemical structure. Lett Appl Microbiol. 2006;43(2):149-54.

58. Tampau A, González-Martínez C, Chiralt A. Release kinetics and antimicrobial properties of carvacrol encapsulated in electrospun poly-(ε-caprolactone) nanofibres: application in starch multilayer films. Food Hydrocoll. 2018;79:158-69.

59. Netopilova M, Houdkova M, Rondevaldova J, Kmet V, Kokoska L. Evaluation of in vitro growth-inhibitory effect of carvacrol and thymol combination against Staphylococcus aureus in liquid and vapour phase using new broth volatilization chequerboard method. Fitoterapia. 2018;129:185-90.

60. Wang L, Fogliano V, Heising J, Dekker M. The effect of pore size on the diffusion of volatile antimicrobials is a key factor to preserve gelled foods. Food Chem. 2021;351:129316.

61. Wang T-H, Hsia S-M, Wu C-H, Ko S-Y, Chen MY, Shih Y-H, et al. Evaluation of the antibacterial potential of liquid and vapor phase phenolic essential oil compounds against oral microorganisms. PLoS One. 2016;11(9):e0163147.

62. Boukhatem MN, Darwish NHE, Sudha T, Bahlouli S, Kellou D, Benelmouffok AB, et al. In vitro antifungal and topical anti-inflammatory properties of essential oil from wild-growing *Thymus vulgaris* (Lamiaceae) used for medicinal purposes in Algeria: a new source of carvacrol. Sci Pharm. 2020;88(3):33.

63. Zhu L, Olsen C, McHugh T, Friedman M, Levin CE, Jaroni D, et al. Edible films containing carvacrol and cinnamaldehyde inactivate *Escherichia coli* O157:H7 on organic leafy greens in sealed plastic bags. J Food Saf. 2020;40(2):e12758.

64. Fonseca LM, Souza EJD, Radünz M, Gandra EA, Zavareze ER, Dias ARG. Suitability of starch/carvacrol nanofibers as biopreservatives for minimizing the fungal spoilage of bread. Carbohydr Polym. 2021;252:117166.

65. Engel JB, Heckler C, Tondo EC, Daroit DJ, Malheiros PS. Antimicrobial activity of free and liposome-encapsulated thymol and carvacrol against Salmonella and Staphylococcus aureus adhered to stainless steel. Int J Food Microbiol. 2017;252:18-23.

66. Zhang D, Gan R-Y, Ge Y-Y, Yang Q-Q, Ge J, Li H-B, et al. Research progress on the antibacterial mechanisms of carvacrol: a mini review. Bioact Compd Health Dis. 2018;1(6):71.